Journal of ELECTRONIC MATERIALS, Vol. 36, No. 12, 2007 Regular Issue Paper
DOI: 10.1007/s11664-007-0245-y
© 2007 TMS

Electrical Characterization of Defects Introduced During Sputter Deposition of Schottky Contacts on *n*-type Ge

F.D. AURET,[1,2] S. COELHO,[1] W.E. MEYER,[1] C. NYAMHERE,[1] M. HAYES,[1] and J.M. NEL[1]

1.—Physics Department, University of Pretoria, Pretoria 0002, South Africa. 2.—e-mail: danie.auret@up.ac.za

The authors have investigated by deep level transient spectroscopy the electron traps introduced in *n*-type Ge during sputter deposition of Au Schottky contacts. They have compared the properties of these defects with those introduced in the same material during high-energy electron irradiation. They found that sputter deposition introduces several electrically active defects near the surface of Ge. All these defects have also been observed after high-energy electron irradiation. However, the main defect introduced by electron irradiation, the V-Sb center, was not observed after sputter deposition. Annealing at 250°C in Ar removed the defects introduced during sputter deposition.

Key words: Germanium, sputter deposition, Schottky contacts, defects, deep level transient spectroscopy (DLTS)

INTRODUCTION

The low effective mass of holes in Ge has opened up the possibility of using Ge in ultrafast complimentary metal-oxide-semiconductor (CMOS) devices.[1] A Ge channel MOSFET has benefits as a performance booster for future scaled CMOS circuits, because it offers higher mobility for electrons and holes than in a Si MOSFET.[2] Thus, Metal Source/Drain MOSFETs (MSD-MOSFETs) with ultra-thin Ge-on-Insulator (GOI) channels have been proposed and realized.[2] This interest in Ge devices, in turn, has sparked renewed interest in the properties of defects in Ge because defects ultimately determine the performance of devices. In recent studies the properties of the defects introduced during high-energy gamma-, electron- and proton irradiation,[3–6] as well as indium-ion implantation,[7] of Ge were reported. The defects introduced during electron beam deposition of Pt Schottky contacts have also been characterized.[8] The investigations of metallization-induced defects are important because it is well known that metallization procedures, e.g. sputtering and electron beam deposition, introduce defects at and close to the metal-semiconductor junction. These defects influence device performance and alter the barrier heights of the contacts.[9,10] The defects responsible for these barrier adjustments are formed when energetic particles reach the semiconductor surface and interact with it, resulting in lattice damage. Depending on the application, these defects may either be beneficial or detrimental for optimum device functioning. For example, for Si it has been shown that the defects introduced during high-energy electron and proton irradiation increase the switching speed of devices.[11]

In this study we report the electronic properties of defects introduced in *n*-type Ge during sputter deposition of Au Schottky contacts. We show that sputter deposition introduces several electron traps and that the electronic properties of these defects are the same as some of the defects introduced during MeV electron irradiation of the same material.

EXPERIMENTAL PROCEDURE

For this experiment we used bulk-grown (111) *n*-type Ge doped with Sb to a level of 2.5×10^{15} cm^{-3}.

(Received February 22, 2007; accepted March 20, 2007; published online September 21, 2007)

Before metallization the samples were first degreased and then etched in a mixture of H_2O_2 (30%): H_2O (1:5) for 1 min. Directly after cleaning they were inserted into a vacuum chamber where AuSb (0.6% Sb) was deposited on their back surfaces as ohmic contacts. The samples were then annealed at 350°C in Ar for 10 min. Before Schottky contact deposition, the samples were again chemically cleaned as described above. Au contacts, 0.63 mm in diameter, were sputter-deposited through a mechanical mask. For sputter deposition Ar was leaked into the system to a pressure of 6×10^{-2} mbar to create the plasma. The accelerating sputter voltage was 700 V and the power was 100 W. The sputter-deposited contacts were deposited at a rate of about 2 nm s^{-1} and were 400 nm thick. "Control" Au Schottky contacts were deposited on identical samples by resistive evaporation—a process known not to introduce defects in semiconductors. Both conventional and high-resolution Laplace DLTS[12,13] were used to study the defects introduced in the Ge during the sputter deposition process.

RESULTS AND DISCUSSION

Room temperature capacitance–voltage (C–V) measurements revealed that the barrier heights of control (resistively deposited) contacts and sputter deposited contacts were 0.44 ± 0.01 eV and 0.45 ± 0.01 eV, respectively. This is the same for all practical purposes and shows that sputter deposition does not introduce defects in a sufficiently high concentration to alter the built-in voltage of the Au-Ge interface. Room temperature current–voltage (I–V) measurements, however, showed that the reverse leakage current of the sputter deposited contact (at −1 V bias) was about an order of magnitude higher (5×10^{-5} A) than that of the resistively deposited contact (2×10^{-6} A). This is illustrated in Fig. 1. This, together with the fact that the C–V Schottky barrier height was not decreased during sputter deposition, suggests that the increase in reverse current is caused by sputter deposition introduced defects that act as recombination-generation centers. We have also measured the reverse current (at −1 V bias) as a function of temperature. Upon cooling, the reverse current of the control diode (at −1 V bias) decreased from 2×10^{-6} A at room temperature to 1×10^{-13} A at 100 K (Fig. 1). The lower current limit of our current (I) measurement system is about 2×10^{-14} A. The reverse current (at −1 V bias) of the sputtered diode, on the other hand, slowly decreased from 5×10^{-5} A at room temperature to 3×10^{-9} A at 100 K, where the reverse current was almost four orders of magnitude higher than that of the control diode (Fig. 1). The fact that the reverse current of the sputtered diode was so much higher than that of the control diode emphasizes the importance of sputter deposition introduced defects as recombination centers, especially at low temperatures.

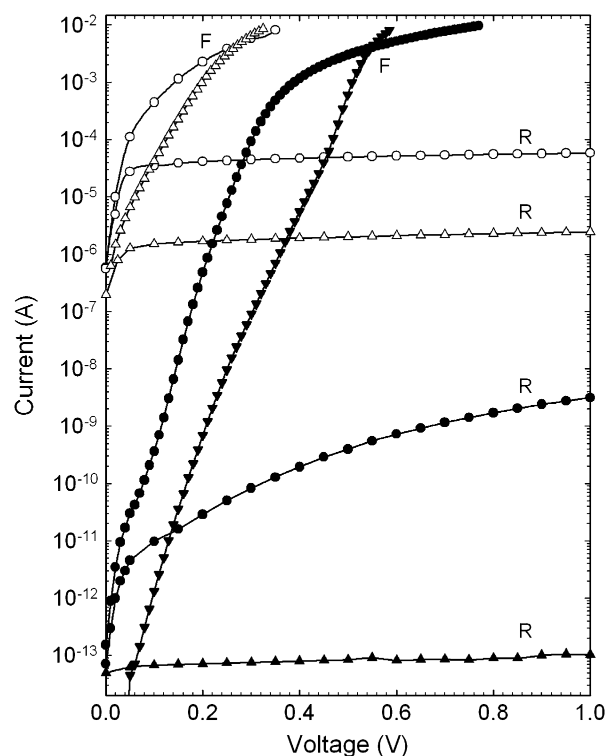

Fig. 1. I–V curves of resistively deposited (*triangles*) and sputter deposited (*circles*) Au Schottky contacts to Ge, recorded at room temperature (*open symbols*) as well as at 100 K (*solid symbols*). Note that the forward 'F' and reverse 'R' currents are plotted in the same quadrant.

In Fig. 2 we depict the DLTS spectra for control and sputter-deposited Au contacts. The DLTS spectrum, curve (a), of the control diode does not contain any detectable DLTS peaks. Curve (b) shows that sputter deposition introduced several electron traps: $ES_{0.14}$, $ES_{0.20}$, $ES_{0.21}$, $ES_{0.24}$, and $ES_{0.31}$. In this nomenclature 'ES' means electron trap induced by sputtering, and the subscript is the activation energy determined from the Arrhenius plots in Fig. 3. The electronic properties of these defects are summarised in Table I. The peaks of $ES_{0.20}$ and $ES_{0.21}$ could only be clearly resolved after using high-resolution Laplace DLTS.[12,13] In Fig. 2 we also compare the DLTS spectrum of sputter-induced defects to those of Au Schottky diodes formed by electron beam deposition (EBD) (curve c) and to the spectrum of Ge irradiated with high energy electrons (curve d).[8] This comparison reveals that, except for the V-Sb center, sputter deposition introduces the same defects as high energy electron irradiation. This is also verified in Fig. 3 where the DLTS signatures of these defects are compared. Interestingly, none of the defects introduced by EBD, except the V-Sb complex, correspond to defects introduced by high-energy electron irradiation or sputter deposition. Unlike in previous studies of high-energy electron irradiated Ge and

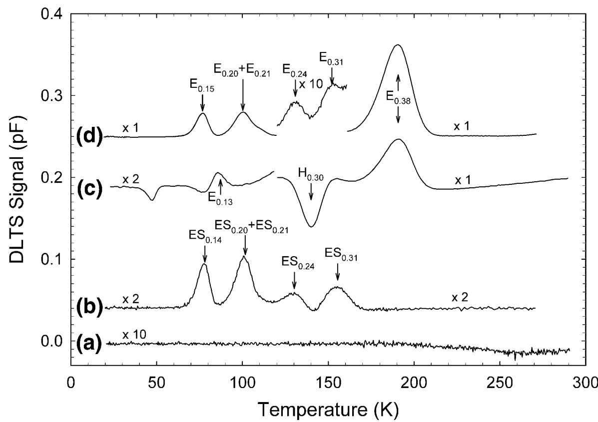

Fig. 2. DLTS spectra of Schottky contacts to *n*-Ge. Curve (a) resistively deposited (control) Au contact; curve (b) sputter deposited Au contact; curve (c) Au contact deposited by electron beam deposition; and curve (d) Pd contact irradiated with MeV electrons.[7] All spectra were recorded using a rate window of 80 s^{-1} at a quiescent reverse bias of –1 V and a pulse, V_p, of 0.15 V into forward bias.

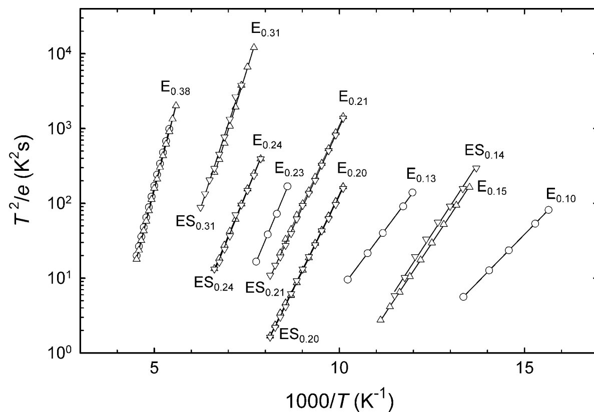

Fig. 3. Arrhenius plots for defects introduced in *n*-type Ge during electron beam deposition (*circles*), sputter deposition (*upside down triangles*) and high-energy electron irradiation induced (*upright triangles*). All data was acquired using the bias and pulsing conditions defined in the caption of Fig. 2.

electron beam deposited (EBD) Schottky diodes,[8] we could not detect any hole traps in the sputter deposited contacts studied here, even when applying a strong forward bias. After irradiating the sputter deposited contacts with MeV electrons the hole traps typical of electron irradiation could be observed. This means that sputter deposition by itself does not introduce any hole traps in detectable concentrations.

The main electron trap introduced by EBD and electron irradiation was the $E_{0.38}$, which was shown to be the (–/–) charge state of the V-Sb center. The fact that this defect is not observed after sputter deposition implies that this process does not introduce a sufficient number of single vacancies at and close to the surface that can diffuse into the Ge and combine with Sb ions to form V-Sb, as in the case of EBD.[8] It should be realised that most of the damage that we observe after sputter deposition is caused by backscattered neutral Ar ions that have a maximum energy of 700 eV. From TRIM[14] modelling we have found that the range and straggle of these ions are 2.1 nm and 1.2 nm, respectively. In the first 3 nm they deposit on average 20 eV/nm to the Ge lattice and produce, on average, 5 vacancies/nm. This implies that defects larger than the single vacancy, e.g. divacancy and vacancy (or interstitial) clusters, can be formed. Whereas vacancy clusters, such as the divacany, are stable at room temperature,[3] interstitial clusters, by nature, are not very stable. It is therefore conceivable that when they break up, interstitials are injected into the Ge during sputter deposition. Based on this we speculate that the defects we observe after sputter deposition are related to interstitial-impurity complexes (e.g. I-Sb), vacancy- or interstitial clusters, or complexes of these clusters with impurities. The signature of $ES_{0.31}$ (similar to that of $E_{0.31}$) is close to that reported for the divacancy ($E_{0.29}$),[3] whereas the signatures of $ES_{0.14}$, $ES_{0.20}$, and $ES_{0.21}$ are close to that of the $E_{0.13}$, $E_{0.19}$, and $E_{0.23}$ proposed to be related to Sb and the Ge interstitial.[3]

As in previous studies on other semiconductors,[8–10] we have found that the defects introduced during sputter deposition of contacts on Ge are located close to the metal-semiconductor interface. A depth profile constructed using the fixed-bias variable-pulse method showed that the concentration of the sputter-induced defects is of the order of 10^{13} cm^{-3} at 100 nm below the interface and decreased exponentially into the Ge. However, it should be pointed out that from TRIM modelling we have found that most of the directly produced sputter damage is located within the first 5 nm below the surface. It is well known that it is not possible to accurately probe defects by DLTS so close to the surface. Therefore, the defects that we observe beyond 100 nm reached that location by diffusion and their concentration is not a fair reflection of that of the defects directly produced by sputter-deposition close to the interface.

We have also investigated the thermal stability of the sputter deposition induced defects by isochronal annealing in argon. After annealing at 150°C for 10 min the $ES_{0.14}$, $ES_{0.20}$, and $ES_{0.24}$ levels could no longer be detected but the concentration of $ES_{0.31}$ increased by about a factor of two. Annealing at 200°C reduced the concentrations of $ES_{0.21}$ and $ES_{0.31}$ by 10% and 30%, respectively, and annealing at 250°C removed them completely, and sputter deposition induced defects could no longer be detected. After annealing at 300°C, no additional defects, i.e. no 'second generation' defects could be observed, indicating that the sputter deposition induced defects did not reconstruct during annealing to form larger defects or different defect complexes. The removal temperature of $ES_{0.31}$ of 250°C is higher than the 180°C reported by Fage-Pedersen et al.[3] for removing the divacancy (with a similar energy level). However,

Table I. Electronic Properties of Prominent Defects Introduced in n-Type Ge During Sputter Deposition and MeV Electron Irradiation of Schottky Contacts

Sputter Deposition				MeV Electron Irradiation				
Defect	E_T (eV)	σ_a (cm^2)	T^a_{peak} (K)	Defect	E_T (eV)	σ_a (cm^2)	T^a_{peak}(K)	Similar Defects / Defect ID
$ES_{0.14}$	E_C–0.14	5.5×10^{-15}	78	$E_{0.15}$	E_C–0.15	2.8×10^{-14}	77	$E^b_{0.13}$, Sb and I related^c
$ES_{0.20}$	E_C–0.20	3.7×10^{-14}	100	$E_{0.20}$	E_C–0.20	1.4×10^{-14}	100	$E^c_{0.19}$, Sb and I related^c
$ES_{0.21}$	E_C–0.21	2.0×10^{-14}	109	$E_{0.21}$	E_C–0.21	3.6×10^{-14}	109	$E^c_{0.21}$, Sb related?^{c}
$ES_{0.24}$	E_C–0.24	3.3×10^{-15}	131	$E_{0.24}$	E_C–0.24	2.5×10^{-15}	131	$E^c_{0.23}$, Sb and I related?^{c}
$ES_{0.31}$	E_C–0.31	1.5×10^{-14}	151	$E_{0.31}$	E_C–0.31	5.0×10^{-14}	150	$E^c_{0.29}$?, V^c_2?
—	—	—	—	$E_{0.38}$	E_C–0.38	1.1×10^{-14}	191	$E^b_{0.377}$, $E^c_{0.37}$, V-Sb (–/–)$^{b, c}$
—	—	—	—	$H_{0.30}$	E_V + 0.30	3.66×10^{-13}	142	$H^b_{0.307}$, $H^c_{0.30}$, V-Sb (–/0)^b

[a] Peak temperature at a rate window of 80 s^{-1}; [b] See Ref. 4; [c] See Ref. 3.

it should be borne in mind that the annealing reported by Fage-Pedersen et al.[3] was performed under zero bias where most of the defects are filled with electrons. In our case $ES_{0.31}$ is close to the surface and hence above the Fermi level during annealing. It has been reported that reverse bias annealing (E-center above the Fermi level) impedes the annealing of E-centers[2]. Annealing at temperatures of up to 300°C is not expected to give rise to Au-Ge interaction, e.g. germanidation, because the Au-Ge eutectic temperature is 361°C.[15]

Finally, it is interesting to note that sputter deposition also introduced several defects in Si.[15] Unlike the case of Ge above, annealing of sputter-deposited Ti-W Schottky contacts to n- and p-type Si introduced several second generation defects.[16] It is also important to point out that annealing at 400°C removed some, but not all, of the sputter-induced defects in Si.[16] However, this comparison between sputter-induced defects in Ge and Si may not be very appropriate because the sputter systems and conditions used for the two experiments were different.

SUMMARY

In summary, we have investigated by deep level transient spectroscopy the electron trap defects introduced in n-type Ge during sputter deposition of Au Schottky contacts. We have compared the properties of these defects with those introduced in the same material during high-energy electron irradiation and have found that sputter deposition introduces several electrically active defects near the surface of Ge. All these defects have also been observed after high-energy electron irradiation. However, the main defect introduced by high-energy electron irradiation, the V-Sb complex, was not observed after sputter deposition. Annealing at 250°C in Ar removed the defects introduced during sputter deposition but annealing at higher temperatures did not introduce any new defects.

ACKNOWLEDGEMENTS

The authors gratefully acknowledge financial support of the South African National Research Foundation. The Laplace DLTS software and hardware used in the research was kindly provided by A.R. Peaker (Centre for Electronic Materials Devices and Nanostructures, University of Manchester) and L. Dobaczewski (Institute of Physics, Polish Academy of Sciences).

REFERENCES

1. R. Hull and J.C. Bean, eds., *Germanium Silicon: Physics and Materials, Semiconductors and Semimetals*, Vol. 56 (San Diego, CA: Academic, 1999).
2. K. Ikeda, T. Maeda, and S. Takagi, *Thin Solid Films* 508, 359 (2006).
3. J. Fage-Pedersen, A. Nylandsted Larsen, and A. Mesli, *Phys. Rev. B* 62, 10116 (2000).
4. V.P. Markevich, A.R. Peaker, V.V. Litvinov, V.V. Emstev, and L.I. Murin, *J. Appl. Phys.* 95, 4078 (2004).
5. V.P. Markevich, I.D. Hawkins, A.R. Peaker, K.V. Emstev, V.V. Emstev, V.V. Litvinov, and L. Dobaczewski, *Phys. Rev. B* 70, 235213 (2004).
6. V.P. Markevich, I.D. Hawkins, A.R. Peaker, V.V. Litvinov, L. Dobaczewski, and J.L. Lindström, *Appl. Phys. Lett.* 81, 1821 (2002).
7. F.D. Auret, S. Coelho, M. Hayes, J.M. Nel, and W.E. Meyer, *Appl. Phys. Lett.* 89, 152123 (2006).
8. F.D. Auret, S. Coelho, M. Hayes, and W. E. Meyer, *Appl. Phys. Lett.* 88, 242110 (2006).
9. F.D. Auret, S.A. Goodman, F.K. Koschnik, J.-M. Spaeth, B. Beaumont, and P. Gibart, *Appl. Phys. Lett.* 74, 2173 (1999).
10. G. Myburg and F.D. Auret, *J. Appl. Phys.* 71, 6172 (1992).
11. D.C. Sawko and J. Bartko, *IEEE Nucl. Sci.* 30, 1756 (1983).
12. L. Dobaczewski, P. Kaczor, I.D. Hawkins, and A.R. Peaker, *J. Appl. Phys.* 76, 194 (1994).
13. L. Dobaczewski, A.R. Peaker, and K. Bonde Nielsen, *J. Appl. Phys.* 96, 4689 (2004).
14. J.F. Ziegler, J.P. Biersack, and U. Littmark, *The Stopping and Range of Ions in Solids*, Vol. 1, ed. J.F. Ziegler (New York: Pergamon, 1985).
15. G. Le Lay, G. Quentel, J.P. Faurie, and A. Masson, *Thin Solid Films* 35, 289 (1976).
16. F.D. Auret and G.M. Matusiewicz, *Vacuum* 35, 195 (1985).